

# Yield stress measurements of aqueous foams in the dry limit

B. S. Gardiner, B. Z. Dlugogorski,<sup>a)</sup> and G. J. Jameson

*ARC Centre for Multiphase Processes, Department of Chemical Engineering, The University of Newcastle, Callaghan NSW 2308, Australia*

R. P. Chhabra

*Department of Chemical Engineering, Indian Institute of Technology, Kanpur 20816, India*

(Received 23 February 1998; final revision received 13 July 1998)

## Synopsis

This paper reports measurements of yield stress of aqueous foams approaching the dry foam limit using a pendulum device. Traditionally, the vane rheometer has been used to measure the yield stress in liquids that exhibit wall slip. However, using the simple and inexpensive pendulum technique, shear rates many orders of magnitudes lower can be achieved. The pendulum was used to observe the change in yield stress for the foam as the gas fraction and bubble size increased. The local gas fraction in the foam was found by measuring the sonic velocity, and the bubble size was determined photographically. Strong support is found for the existence of a true yield stress in aqueous foams at the dry foam limit. Yield stress results, once scaled by  $\sigma/\langle R \rangle$ , agree well with data from previous studies. © 1998 The Society of Rheology. [S0148-6055(98)01006-2]

## I. INTRODUCTION

Aqueous foams, although formed from the simple ingredients of a gas and a surfactant solution, exhibit many unusual properties. One of these, usually associated with solids, is the appearance of a yield stress above a critical gas fraction. This yield stress arises due to the internal structure of foam, which consists of bubbles separated by a matrix of thin films. As with some other aspects of foam rheology, such as shear modulus and osmotic pressure, the yield stress of foams is largely dependent on the foam gas fraction (volume of contained gas/volume of foam), surface tension, and bubble size. Previous studies on foams and concentrated emulsions indicate that the yield stress of foams rises sharply with the gas fraction [Wenzel *et al.* (1970); Princen (1985); Calvert and Nezhati (1987); Yoshimura *et al.* (1987); Khan *et al.* (1988)]. Furthermore, when scaled by  $(\sigma/\langle R \rangle)$ , the yield stress increases monotonically with the gas fraction, suggesting that the absolute yield stress increases with increasing surface tension and decreasing bubble size.

There is still some uncertainty about the existence of yield stress in fluids. It has been suggested by Barnes and Walters (1985) that the apparent observed yield stress is a direct function of limitations imposed by the low shear rates available with the rheometer used in the experiments. They conclude that for shear rates which are sufficiently low, all

---

<sup>a)</sup>Author to whom all correspondence should be addressed. Electronic mail: cgbzd@alinga.newcastle.edu.au

fluids will show Newtonian behavior, but sufficient time must be allowed for yield to occur. A practical definition of yield stress or dynamic yield stress is then determined by whether or not yield occurs in the time scale of the application or process. From this standpoint, the concept of a yield stress is a useful idealization. However, despite previous concerns, there is strong experimental and theoretical support for the proposition that a true yield stress exists in fluids with an internal structure, such as foams, concentrated emulsions, and suspensions [Kraynik (1988)]. The interlocking macrostructure of these fluids requires an energy barrier to be overcome before flow, or relative motion within the macrostructure, can occur [Sollich *et al.* (1997); Kraynik and Hansen (1987); Bolton and Weaire (1992); Hutzler *et al.* (1995); Reinelt and Kraynik (1996); Durian (1997)].

One of the main difficulties with studying aqueous foam rheology, and the yield stress in particular, is the inherent instability of foams. Immediately after a foam is produced, the liquid contained within it proceeds to drain out due to gravity, thereby on average increasing  $\phi$  and producing a liquid hold-up gradient within the foam. Furthermore, the process of Ostwald ripening occurs due to gas transfer between bubbles of differing internal pressure. The result of Ostwald ripening is that the average bubble size increases with time, so the properties of the foam may be time dependent. Thus, some of the most reliable experimental work on foam rheology has been done using concentrated emulsions, where diffusion between bubbles is greatly reduced and the relative densities between phases can be controlled to reduce drainage or creaming [Princen (1985); Yoshimura *et al.* (1987)]. In this paper, however, our interests lie in the direct investigation of aqueous foam rheology.

It is apparent that there are two conflicting effects in all foam yield stress measurements. Increases in the gas fraction due to drainage tends to raise the yield stress, whereas increases in the bubble size leads to a reduction in the yield stress. The gas fraction and bubble sizes are generally changing in time. If we want to determine whether foams have a yield stress then we have to allow a long time (low shear rate), and during this waiting time, the properties of the foam may be changing. From this perspective, one of the main challenges in this study was to determine whether foams can be said to possess a true yield stress. The experiments required very low shear rates and a full characterization of the foam over its entire life span, in terms of gas fraction and the average bubble size. For this reason, while using the pendulum device, we determined both the gas fraction and the bubble size of foams experiencing drainage and Ostwald coarsening.

In this paper we describe a pendulum device for measurement of the foam yield stress, along with the results of these measurements. The methods used to characterize the change in gas fraction and bubble size of the evolving foam are also outlined. The present results are placed in the perspective of the data from previous studies.

## II. FOAM GENERATOR AND DIAGNOSTIC TECHNIQUES

Foam examined in this study was produced in a compressed-air foam system described elsewhere [Gardiner *et al.* (1998)]. In brief, a surfactant solution containing elements common to the so-called class-B fire-fighting foam is mixed with compressed air in a static mixer. The surfactant solution is formed by mixing 3 parts of foam concentrate solution with 97 parts of deionized water. The composition of the foam concentrate solution is given in Table I. The static mixer consists of a T junction filled with compacted steel wool. The foam is then passed along 10 m of flexible rubber tubing, which acts as a foam improver. The resulting foam is characterized by a very uniform bubble size of radius  $\sim 140 \mu\text{m}$ . In addition to the narrow bubble size distribution, which

**TABLE I.** Composition of the foam concentrate solution used in the generation of the aqueous foams. This concentrate was mixed with deionized water in a volume ratio of 3:97.

Chemical	Trade name	% by weight	Function
Fluro-alkyl surfactant	FC-100	12	Surfactant
Phenyl sulfate surfactant	Triton X-305	11	Surfactant
Sodium octyl sulfate	...	13	Surfactant
Diethylene otycol monobutyl ether	...	9	Stabilizer
Water	...	55	Solvent

reduces the rate of Ostwald ripening, another advantage of this method of foam production is that the initial value of the gas volume fraction  $\phi$  can be accurately controlled through the use of flow meters located prior to the static mixer.

Since the yield stress of foams depends strongly on  $\phi$ ,  $\langle R \rangle$ , and  $\sigma$ , it was important to characterize the foam throughout the duration of the experiment. Thus, the bubble size was measured using a charge-coupled device camera. Images were captured at certain time intervals during the foam drainage process to give details on how the bubble size changed with time during the experiments. The scale of each image was calibrated by a graduated microscope slide placed at the inside wall of the container. Bubble sizes were characterized by the area of the bubble surface in contact with the viewing surface. As the bubbles were not spherical, an equivalent radius was obtained for each bubble by equating the bubble surface area in contact with the viewing surface to the surface area of a circle. The assumption was made that the area-mean bubble size thus found is an adequate representation of the bulk bubble size, as has been found previously by Cheng and Lemlich (1983). An example of the increase over time of the average bubble radius calculated in this way is shown for the present foam system in Fig. 1.

The average  $\phi$  within the draining foam can be obtained from the volume of liquid drained from the foam. However, as there is a large nonlinear gradient in  $\phi$  with height [Weaire *et al.* (1995); Verbist *et al.* (1996)], the average  $\phi$  poorly reflects the true or local  $\phi$  at any given height in the foam. To examine the yield stress of the foam at the height of the pendulum bob the local  $\phi$ , rather than the average, is required. Model predictions based on the solution to partial differential equations are able to give time evolution of hold-up profiles for a free-draining foam [Bhakta and Ruckenstein (1995); Gururaj *et al.* (1995); Verbist *et al.* (1996)]. However, these predictions are not yet accurate enough for the purpose of this investigation, necessitating an experimental determination of the gas fraction gradient.

To obtain the local  $\phi$  at any height, the variation of the speed of sound with  $\phi$  may be utilized. The sonic velocity in foam is, in general, less than that in its two main components, air and water, considered separately. Previous studies of sound speed in foam [Orenbakh and Shushkov (1992, 1993); Tolstov (1992); Vafina *et al.* (1992); Shushkov *et al.* (1993); Goldfarb *et al.* (1994)] have not been concerned with linking sound velocity to the drainage profiles, concentrating instead on predicting the attenuation of sound in the foams. Our work shows that measurements of the sound velocity is a valuable technique for studying changes in the foam gas fraction.

By treating the foam as a mixture of a compressible gas obeying the ideal gas law and an incompressible liquid, the following equation can be readily obtained [Wood (1941)] as a first-order approximation to the sound speed in foams for the range of  $\phi$  considered in our experiments:

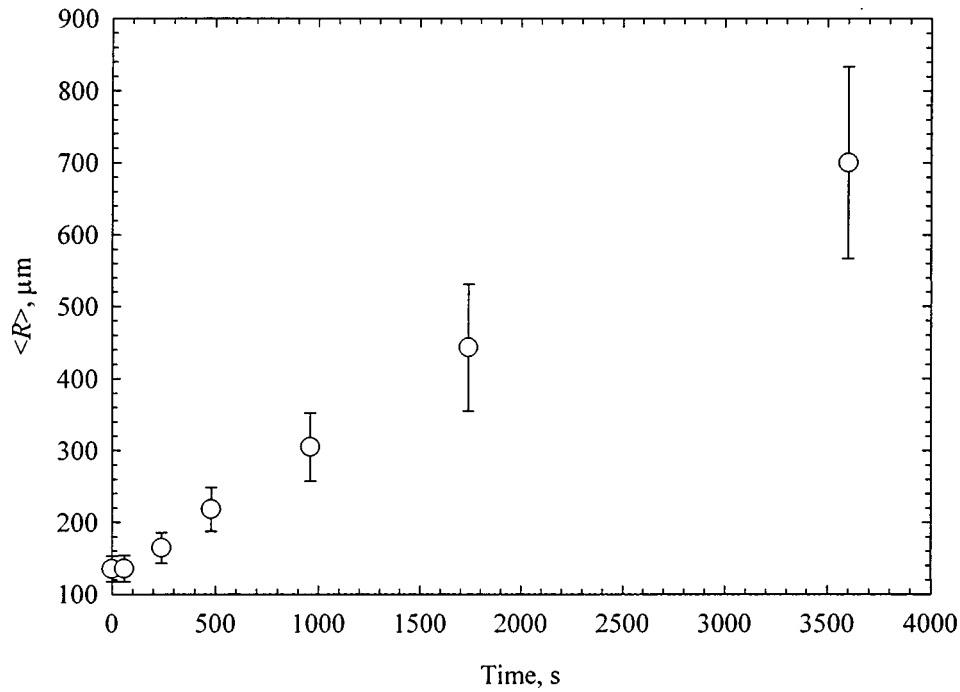


**FIG. 1.** Bubble growth with time for a foam starting with a gas fraction of 0.95; bubble size recorded at  $h/H = 0.5$ . Error bars represent the sum of the standard error associated with sampling size and errors associated with measurement precision.

$$c^2 = \frac{NP}{\rho_L} \frac{1}{(1-\phi)\phi}, \quad (1)$$

where  $N$  is the polytropic expansion exponent.

In our experiments, the sonic velocity in the foam was simply obtained by placing two microphones and a speaker into the foam and recording the time interval between the detection of a short ( $\sim 500 \mu\text{s}$ ) window of oscillations at  $\sim 3400 \text{ Hz}$  from the speaker, at the two microphones, as shown in Fig. 2. The microphone separation was typically 65 mm. This method of measuring the local  $\phi$  was first verified by recording the speed of sound in air, and then in foams of known  $\phi$ . The range of  $\phi$  which the foam generator was capable of producing was limited to 0.8–0.97. (At higher void fractions, the foam tended to collapse within the foam improver.) This limitation has been reported elsewhere in other foam systems [Enzendorfer *et al.* (1995)]. As can be seen from Fig. 3, the agreement between Eq. (1) and the experimental data was excellent. Consequently, where required, Eq. (1) was used to calculate the gas fraction from the measured sonic velocity in the foam. Note that a large variation in  $c$  occurs for  $\phi$  greater than 0.97, and therefore, as the dry foam limit is approached,  $\phi$  is less sensitive to  $c$ .

Using the measurement of the speed of sound in foam, the drainage profile, or the variation of  $\phi$  with height in the foam, can be characterized as a function of time, enabling the gas fraction at the height of the pendulum bob to be known at any time. Figure 4 shows the temporal drainage profile of the foam found in this study. It is seen

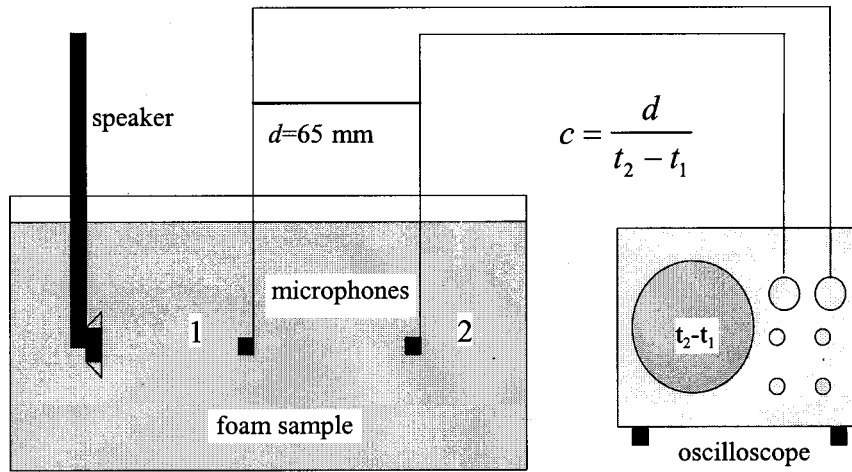


FIG. 2. Determination of the speed of sound in foams of various gas fractions. These results are later used to establish gas fraction gradients within an evolving foam.

that initially the gas fraction is uniform with height. However, as drainage begins the top of the foam rapidly becomes dry. This behavior is progressively followed at lower levels in the foam.

This observation can easily be understood in terms of the conservation of liquid draining through the foam. At some height in the foam  $h$ , the local gas fraction reflects the balance between the liquid flowing out to lower levels below and liquid flowing in

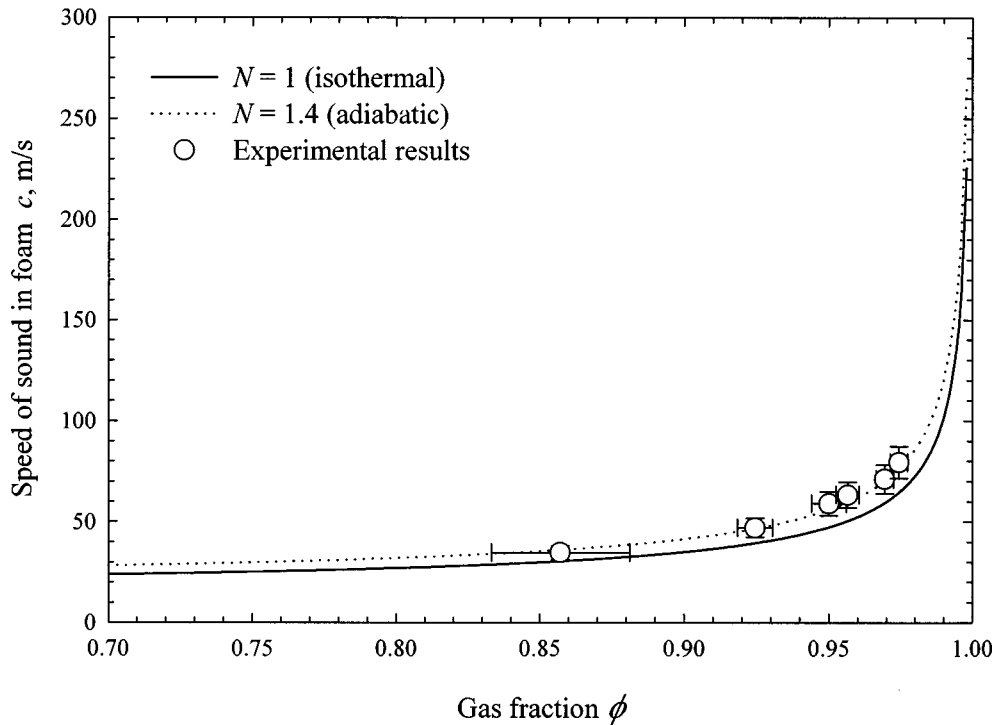


FIG. 3. Verification of the method of sound speed measurement with gas fraction following Eq. (1).

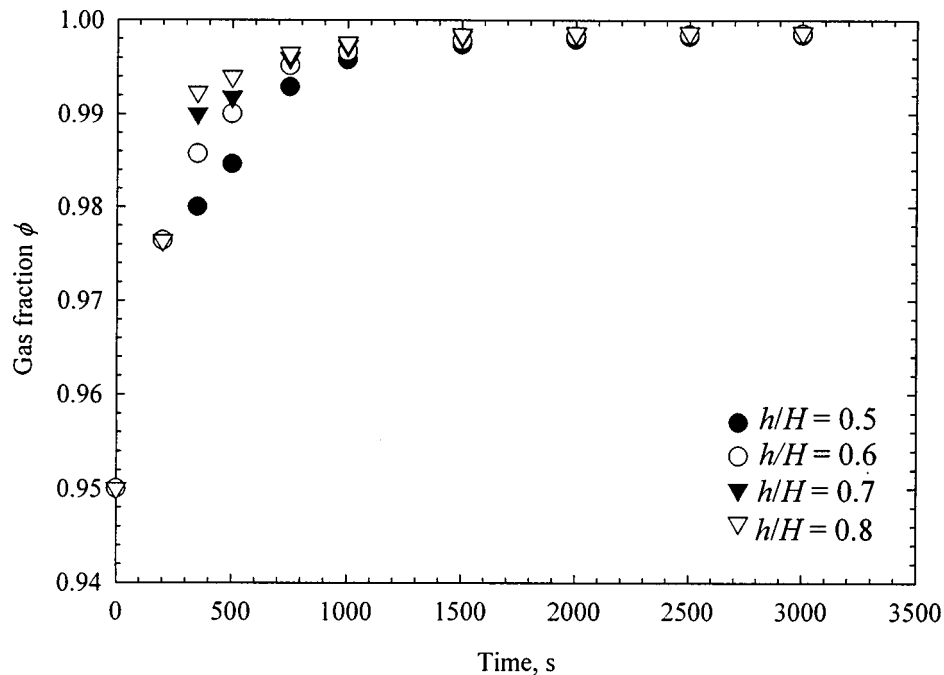


FIG. 4. Drainage profiles for the foam used in this study as determined from the local sound speed measurements;  $h/H$  is the height in the foam, normalized with respect to the initial foam height  $H$ .

from higher levels above. Near the top of the foam, where  $h/H \rightarrow 1$ , there is no liquid flowing in from above. Hence, the gas fraction of the foam at the top rapidly increases and the foam becomes dry. The depletion front of liquid flowing in from higher levels progressively moves down through the foam. Finally, the gas fraction at all heights studied approaches a uniform value. At this point the capillary and gravitational forces are essentially in balance.

### III. EXPERIMENTAL APPARATUS AND RELATED THEORY

The pendulum method for measuring yield stress was first introduced by Uhlherr and co-workers, who used a spherical bob in solutions of carbopol; see, for example, Guo and Uhlherr (1996). If a freely suspended pendulum is released above the surface of a fluid at a finite angle from the vertical, it will fall until gravitational forces are balanced by buoyancy and shear forces acting on the pendulum bob. For a yield stress fluid the final equilibrium angle of the pendulum is nonzero, that is, away from vertical. The equilibrium angle can then be related back to the yield stress. In this work, although the pendulum has mass, the viscous drag is such that the bob does not oscillate freely about the axis of the suspension system. Rather, it is brought to rest before it reaches the lowest possible extremity of the motion, and the yield stress can then be simply related to the equilibrium angle.

In this experiment, a thin flat plate was used for the pendulum bob, orientated so that its long sides are parallel to the direction of motion of the pendulum. A thin plate was selected in place of the spherical bob used by earlier workers to minimize the surface area of the bob in the direction normal to the motion, so that the normal forces on the bob in this direction could be neglected. We estimate the magnitude of the normal forces to be

**TABLE II.** Dimensions, densities, and materials for the components of the pendulum.

Component	Length	Width diameter	Thickness/ internal diameter	Density	Material
(1) Bob	50 mm	25 mm	1 mm	1273 kg/m <sup>3</sup>	Stiff plastic
(2) Tubing	150 mm	2 mm	1 mm	2540 kg/m <sup>3</sup>	Aluminum
(3) Bearing	50 mm	10 mm	9 mm	2540 kg/m <sup>3</sup>	Aluminum

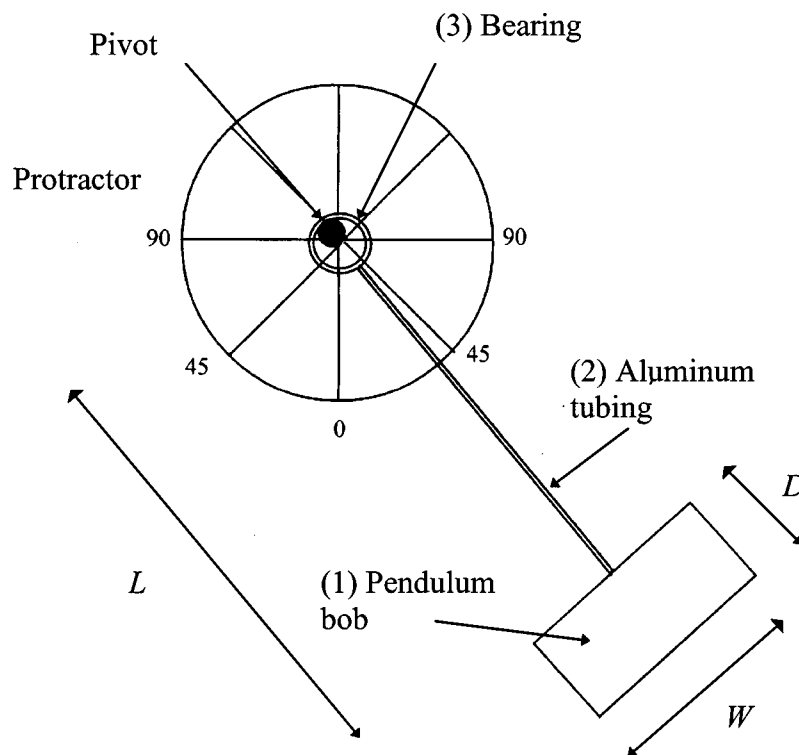
below 3.5% of the forces due to yield stress. The plate surface was roughened to minimize wall slip. With reference to Table II and Fig. 5, the bob (1) was attached to a length of thin-walled aluminum tubing (2), which was in turn connected to aluminum tubing (3) of a larger diameter, which acted as a low friction bearing.

The equation of motion for our physical pendulum moving through a viscous fluid is

$$I \frac{d^2 \theta}{dt^2} = -Mgd \sin \theta + \tau 2WD \left( L + \frac{D}{2} \right), \quad (2)$$

where

$$\tau = \tau \left( \tau_y, \frac{d\theta}{dt}, \eta \right) = \tau_y + F \left( \frac{d\theta}{dt}, \eta \right), \quad (3)$$

**FIG. 5.** Pendulum design; labels indicate components listed in Table II.

and the function  $F$  is specified by a relevant constitutive equation;  $\tau$  denotes the average shear stress acting on the two sides of the bob,  $\tau_y$  is the yield stress, and  $I$  represents the moment of inertia of the pendulum.

The stress due to the fluid on the aluminum tubing has been neglected in Eq. (2) because a large fraction of the tube length is above the foam surface, and the surface area of the submerged tube is much smaller than that of the pendulum bob. However, one can argue that the yield stress of foams is expected to increase with the foam gas fraction, and the gas fraction should be the greatest near the foam top surface, where the tube is in contact with the foam. For this reason, the validity of our assumptions was verified experimentally by varying the length of tubing submerged in the foam, as discussed further in the results and discussion section.

The distance between the center of mass and the pivot point for our system geometry is found to be

$$d = \frac{M_{\text{eff}}(2L+D) + M_a L - \rho_f \pi R_a^2 L_s (2L - L_s)}{2M}, \quad (4)$$

where

$$M_{\text{eff}} = (\rho_b - \rho_f) D W T.$$

The effect of the bearing at the pivot point is neglected as the close proximity of the bearing to the pivot produces negligible additional torque. Therefore, Eq. (2) becomes

$$I \frac{d^2 \theta}{dt^2} = - \frac{g \sin \theta}{2} [M_{\text{eff}}(2L+D) + M_a L - \rho_f \pi R_a^2 L_s (2L - L_s)] + \tau 2 W D \left( L + \frac{D}{2} \right). \quad (5)$$

When the bob encounters the foam, it slides gently to rest, and the steady-state solution to Eq. (5) that is for

$$\frac{d\theta}{dt} = 0, \quad \frac{d^2 \theta}{dt^2} = 0, \quad (6)$$

is determined by pendulum geometry and the yield stress only, and is independent of the pendulum moment of inertia. Hence, from Eqs. (3), (5), and (6),

$$\tau_y = g \sin \theta \frac{[M_{\text{eff}}(2L+D) + M_a L - \rho_f \pi R_a^2 L_s (2L - L_s)]}{2 W D (2L + D)}. \quad (7)$$

The angle of the pendulum  $\theta$  was measured using a protractor. The height of the foam changes with time due to the collapse of bubbles at the top of the foam because of the thinning of lamellae and breakage caused by evaporation and drainage. Therefore, the height of foam with time was also recorded. Care was taken to minimize vibrations.

#### IV. RESULTS AND DISCUSSION

A number of preliminary tests were undertaken to evaluate the system. First, the pendulum motion was examined with a viscous Newtonian fluid, glycerol. In this case, the pendulum fell to a vertical position as would be expected of a liquid showing no yield stress. The time to reach equilibrium was approximately 3 min. Note that the apparent loss in weight of the bob is much larger in glycerol than in the foam, which has a density close to that of air.

Although most of the following experiments were performed over a period of an hour, we initially allowed the pendulum motion to progress for a 24 h period in a covered



container to reduce evaporative bubble rupture. After 24 h, the pendulum remained at a reproducible nonzero angle of  $10^\circ$ . The time scale of this measurement ( $\sim 10^5$  s) is much longer than that when the vane rheometer is used to measure the yield stress.

Clearly, it seems that at least for very dry foams, a yield stress is a real phenomenon. After about 2 h very little liquid drains from the foam, the loss of liquid due to evaporation is minimized, and hence, the gas fraction of the foam is relatively constant during the time period between 2 and 24 h. Therefore, the only change in the foam is the increase in bubble size from approximately 1 to 7.5 mm, with a corresponding decrease in the angle from  $18^\circ$  to  $10^\circ$ . After 24 h, the yield stress is 1.5 Pa. If this dry foam result is then scaled by  $\sigma/\langle R \rangle$  with  $\sigma = 20$  mN/m, the resulting scaled yield stress is 0.56. Incidentally, this scaled yield stress is of the same order of magnitude as the predictions from the various two-dimensional and three-dimensional models of dry foam [Stamenovic and Wilson (1984); Stamenovic (1991); Bolton and Weaire (1992); Hutzler *et al.* (1995); Reinelt and Kraynik (1996)].

Other preliminary tests included dropping the pendulum from different heights above the foam surface, ranging from just above the surface, to 5 cm above the foam. It was found that the height of drop had no effect on the final position of the pendulum or the rate at which the pendulum moved through the foam. Apparently, the pendulum is decelerated very rapidly by the foam matrix.

Another interesting observation is that if the pendulum is removed after a time of the order of 30 min, when it has reached a stable angle, and is then dropped again in the foam at a different site, it returns to the same angle within 2–3 min.

These observations suggest that the motion of the pendulum is governed by the change in yield stress with a changing foam structure, that is, with the evolution of gas fraction and bubble size in time, and not by the lack of a yield stress. Thus, the angle at any instant reflects the dynamic yield stress of the particular foam structure, which exists at that time in the vicinity of the bob. This is a very useful result as it allows the yield stress of a foam to be examined over a range of gas fraction and bubble sizes by assuming quasistatic equilibrium.

The foam height was varied to see if there was any significant effect of the partly submerged aluminum tubing on the observed yield stress. The initial void fraction  $\phi$  was maintained at 0.95. The experimental results are plotted in Fig. 6. Different foam heights correspond to different submerged pendulum wire lengths. After calculating the yield stress for the local foam density at the height of the pendulum bob, no dependence on initial foam height was seen, as is illustrated in Fig. 7, which was obtained from the data presented in Fig. 6. This result confirms the assumption made in the experimental section that the yield stress on the submerged aluminum wire may be neglected.

It is found that after 40 min the liquid drainage from the foam has almost ceased, indicating a significant reduction in the rate of change of the foam gas fraction. The sound velocity measurements shown in Fig. 4 also support this conclusion. From this time onwards the final angle of the pendulum is almost independent of the foam height at  $\sim 20^\circ$ , see Fig. 6.

In Fig. 7 the yield stress is plotted as a function of gas fraction for various initial foam heights. All the data shown in Fig. 7 were obtained after 4 min had elapsed from the release of the pendulum to ensure that a quasistatic equilibrium angle had been reached and that any effect due to differences in the initial foam height was removed.

Two distinct regions can be seen in Fig. 7. The first, starting at  $\phi = 0.975$ , exhibits a gradual decrease in yield stress with increasing gas fraction. Although at first surprising, the decrease in yield stress is readily explained by considering the interplay of the competing effects of drainage of the liquid films and increase in the bubble size on the foam

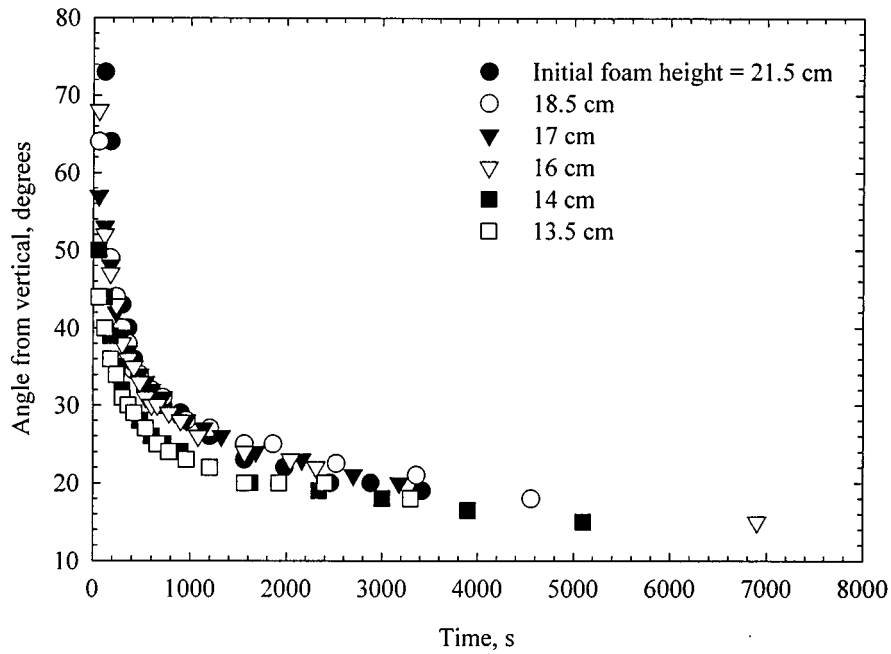


FIG. 6. Combination of pendulum temporal angular position for various initial foam heights.

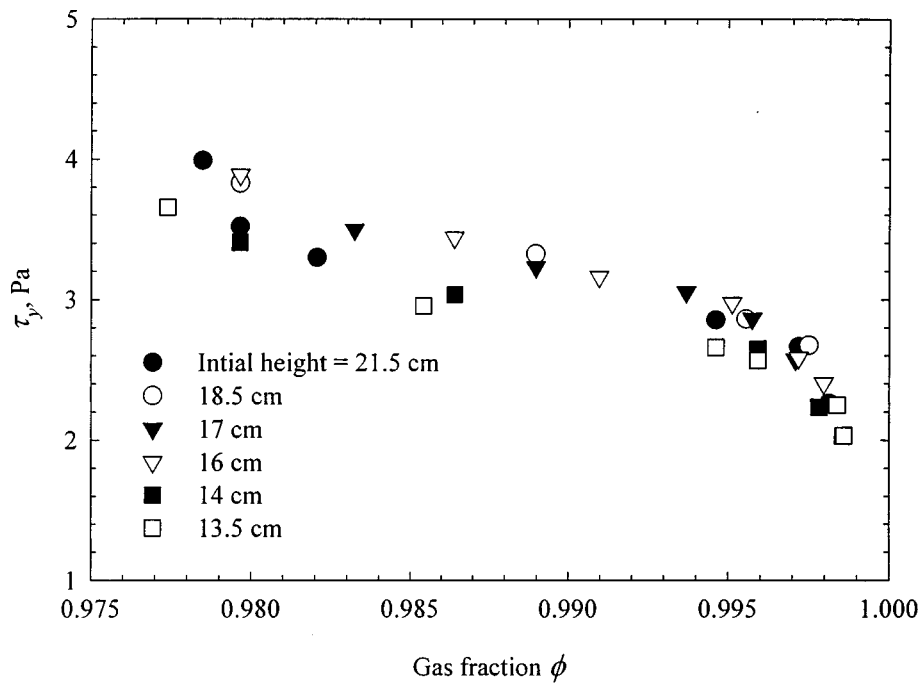


FIG. 7. The results for various initial foam heights combined to reveal the trend of yield stress variation with gas fraction. The unexpected result of decreasing yield stress with an increasing gas fraction is due to a changing bubble size, see Fig. 1.

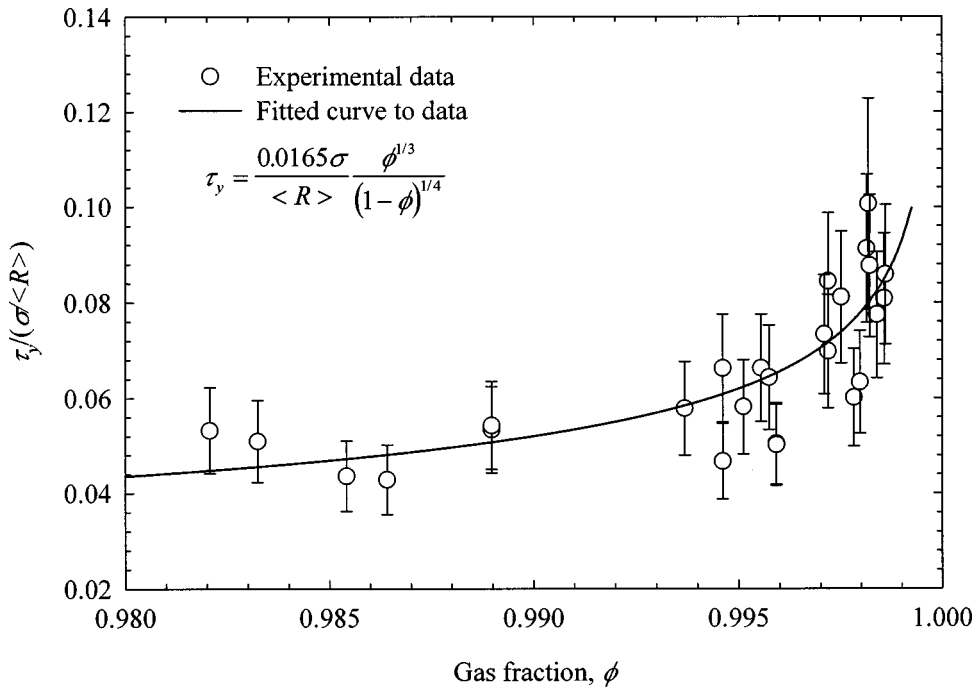


FIG. 8. Once bubble size effects have been accounted for, the yield stress is seen to increase with gas fraction as expected from previous studies.

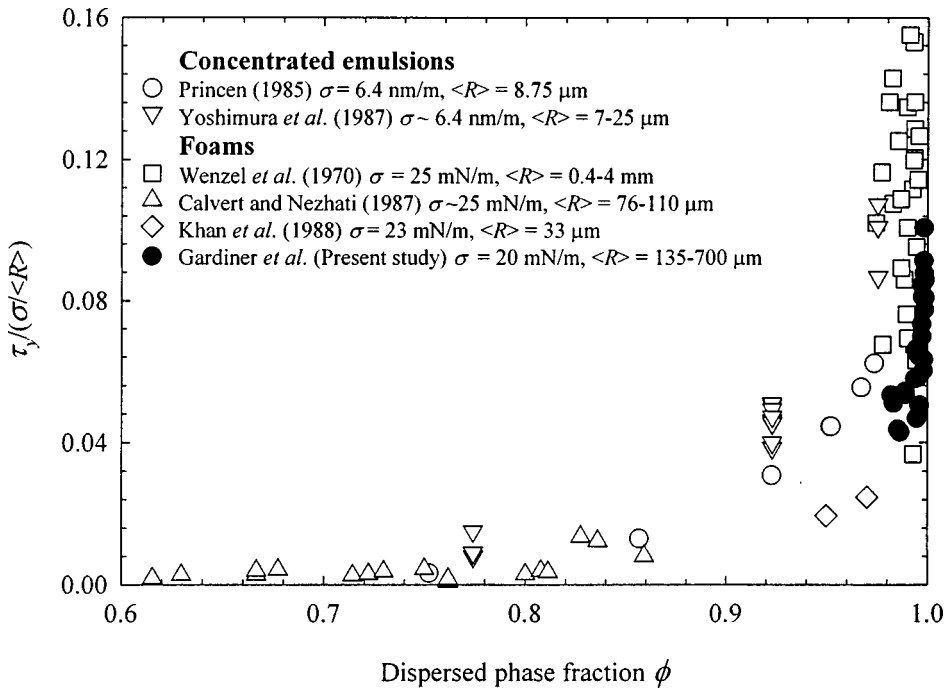


FIG. 9. Comparison of previous author's results with the present study; all data are scaled by  $\sigma/\langle R \rangle$ . Our estimate of  $\tau_y/(\sigma\langle R \rangle) = 0.56$  for  $\phi \cong 1$  is not included in the graph to obtain a better resolution for low values of  $\tau_y/(\sigma\langle R \rangle)$ .

yield stress. The second region is identified by a rapid decline in the yield stress at high gas fractions. These conditions arise when the foam has become aged, the films have thinned to the point of rupture, and the rate of drainage in the films has become very small. The major change in the foam structure is then brought about simply by growth in the mean bubble size due to film rupture and coalescence. When the films rupture the number of films which are cut by any arbitrary horizontal surface in the foam is reduced, but the thickness of the individual films will increase for a short time, allowing drainage to resume and the gas fraction to continue to increase.

The data shown in Fig. 7 appear to suggest that the yield stress decreases with increasing void fraction, whereas it is known that the  $\tau_y$  for a given foam actually increases with increasing  $\phi$ . However, the effect of changes in the bubble size have not yet been accounted for. If the yield stress data collected are scaled by  $\sigma/\langle R \rangle$  and displayed as in Fig. 8, the general behavior is as expected. The scaled yield stress increases with increasing gas fraction. It is clearly important for measurements of the foam yield stress to be accompanied by accurate recordings of the bubble size and of the surface tension to avoid the wrong conclusions being drawn.

In Fig. 9, the scaled results of the present investigation are compared directly to the scaled results of previous studies on foams and concentrated emulsions. A range of techniques have been employed in these studies. No discernible difference in the observed yield stress can be traced to the method used. Figure 9 shows considerable scatter in previous experimental studies due to experimental uncertainty and perhaps variations in the characteristics of foam samples such as polydispersity. However, it is clear that the results of the present study fall within the range of the previous investigations. In particular, it is seen that when scaled by a  $\sigma/\langle R \rangle$ , all of the results, including those from this investigation, lie on a curve characterized by an increasing yield stress with an increasing gas fraction.

## V. CONCLUSION

Through the use of a very simple experimental design involving a moving pendulum, the yield stress in a foam can be determined as a function of the gas fraction and the bubble size. There is a strong indication that a true yield stress exists at the dry foam limit. The observed yield stress is strongly dependent on gas fraction and bubble size. The present results agreed well with previous studies on aqueous foams and concentrated emulsions when scaled by  $\sigma/\langle R \rangle$ , indicating the possible equivalence of the yield rheology of aqueous foams and concentrated emulsions. The scatter of experimental data from the present and prior studies tends to suggest that other factors not included in the analysis, such as bubble size distribution, may play a role in determining foam yield stress.

## ACKNOWLEDGMENTS

The authors would like to thank Tim Budden for his help with measuring the speed of sound in foams, and Ted Schaefer of 3M Australia for providing the generic foam concentrate.

## NOMENCLATURE

$c$	Sonic velocity (m/s)
$D$	Dimension of bob in direction parallel to main axis of pendulum (m)
$d$	Distance between the center of mass and pivot (m)

$F$	Shear function, dependent on foam constitutive equation (Pa)
$g$	Acceleration due to gravity ( $\text{m/s}^2$ )
$H$	Total foam height (m)
$h$	Height within foam (m)
$I$	Moment of inertia ( $\text{kg m}^2$ )
$L$	Length of aluminum tubing (m)
$L_s$	Submerged length of aluminum tubing (m)
$M$	Effective total mass of partly submerged pendulum (kg)
$M_a$	Mass of aluminum tubing (kg)
$M_b$	Mass of bob (kg)
$M_{\text{eff}}$	Effective mass of the submerged bob (kg)
$m$	Mass element at distance $r$ from pivot (kg)
$N$	Polytropic exponent (—)
$P$	Atmospheric pressure (Pa)
$R$	Bubble radius (m)
$r$	Radial distance from pivot (m)
$\langle R \rangle$	Average bubble radius (m)
$R_a$	Radius of aluminum tubing (m)
$T$	Thickness of pendulum bob (m)
$t$	Time (s)
$W$	Dimension of bob perpendicular to main axis of pendulum in the direction of motion (m)
$\phi$	Volume gas fraction in foam or dispersed phase fraction in emulsions (—)
$\eta$	Foam viscosity (Pa s)
$\theta$	Angle at which the line separating the pivot and center of mass is away from vertical (—)
$\rho_f, \rho_L, \rho_b, \rho_{al}$	Density of foam, foam solution, pendulum bob, aluminum tubing, respectively ( $\text{kg/m}^3$ )
$\sigma$	Surface tension (N/m)
$\tau$	Total stress on pendulum bob (Pa)
$\tau_y$	Foam yield stress (Pa)

## References

- Barnes, H. A. and K. Walters, "The Yield Stress Myth?," *Rheol. Acta* **24**, 323–326 (1985).
- Bhakta, A. and E. Ruckenstein, "Drainage of a Standing Foam," *Langmuir* **11**, 1486–1492 (1995).
- Bolton, F. and D. Weaire, "The Effects of Plateau Borders in the Two-Dimensional Soap Froth. II. General Simulation and Analysis of Rigidity Loss Transition," *Philos. Mag. B* **65**, 473–487 (1992).
- Calvert, J. R. and K. Nezhati, "Bubble Size Effects in Foams," *Int. J. Heat Fluid Flow* **8**, 102–106 (1987).
- Cheng, H. C. and R. Lemlich, "Errors in the Measurement of Bubble Size Distribution in Foam," *Ind. Eng. Chem. Fundam.* **22**, 105–109 (1983).
- Durian, D., "Bubble-Scale Model of Foam Mechanics: Melting, Nonlinear Behavior, and Avalanches," *Phys. Rev. E* **55**, 1739–1751 (1997).
- Enzendorfer, C., R. A. Harris, P. Valko, M. J. Economides, P. A. Fokker, and D. D. Davies, "Pipe Viscometry of Foams," *J. Rheol.* **39**, 345–358 (1995).
- Gardiner, B. S., B. Z. Dlugogorski, and G. J. Jameson, "Rheology of Fire-Fighting Foams," *Fire Safety J.* **31**, 61–75 (1998).
- Goldfarb, I. I., I. R. Shreiber, and F. I. Vafina, "On the Experiment of Determining the Sound Velocity in a Foam," *Acustica* **80**, 583–586 (1994).
- Guo, Y. and P. H. T. Uhlherr, "Static Yield Stress using a Pendulum with Cylindrical Bob," *Proceedings of the XIIIth International Congress on Rheology, Quebec City, Canada*, 731–731 (1996).

- Gururaj, M., R. Kumar and K. S. Ghandi, "A Network Model of Static Foam Drainage," *Langmuir* **11**, 1381–1391 (1995).
- Hutzler, S., D. Weaire and F. Bolton, "The Effects of Plateau Borders in the Two-Dimensional Soap Froth. III. Further Results," *Philos. Mag. B* **71**, 277–289 (1995).
- Khan, S. A., C. A. Schnepfer and R. C. Armstrong, "Foam Rheology. III. Measurement of Shear Flow Properties," *J. Rheol.* **31**, 69–92 (1988).
- Kraynik, A. M., "Foam Flows," *Annu. Rev. Fluid Mech.* **20**, 327–357 (1988).
- Kraynik, A. M. and M. G. Hansen, "Foam Rheology: A Model of Viscous Phenomena," *J. Rheol.* **31**, 175–205 (1987).
- Orenbakh, Z. M. and G. A. Shushkov, "Velocity and Dissipation of Sound in Gas–Liquid Foams," *Sov. Phys. Acoust.* **38**, 204 (1992).
- Orenbakh, Z. M. and G. A. Shushkov, "Acoustical Characteristics of Water–Air Foams," *Acoust. Phys.* **39**, 63–66 (1993).
- Princen, H. M., "Rheology of Foams and Highly Concentrated Emulsions II. Experimental Study of the Yield stress and Wall Effects for Concentrated Oil-in-Water Emulsions," *J. Colloid Interface Sci.* **105**, 150–171 (1985).
- Reinelt, D. A. and A. M. Kraynik, "Simple Shearing Flow of a Dry Kelvin Soap Film," *J. Fluid Mech.* **311**, 327–343 (1996).
- Shushkov, G. A., V. N. Feklistov, K. B. Kann and Z. M. Orenbakh, "Effect of the Structure and Properties of Foams on Propagation of Sound in them. The Sound Velocity," *Kolloidn. Zh.* **55**, 136–140 (1993).
- Sollich, P., F. Lequeux, P. Hébraud and M. Cates, "Rheology of Soft Glassy Materials," *Phys. Rev. Lett.* **78**, 2020–2023 (1997).
- Stamenovic, D. and T. A. Wilson, "The Shear Modulus of Liquid Foam," *Trans. ASME, J. Appl. Mech.* **51**, 229–231 (1984).
- Stamenovic, D., "A Model of Foam Elasticity Based upon the Laws of Plateau," *J. Colloid Interface Sci.* **145**, 255–259 (1991).
- Tolstov, G. S., "Propagation of Acoustic Waves in Foams," *Sov. Phys. Acoust.* **38**, 596–600 (1992).
- Vafina, F. I., I. I. Gol'dfarb and I. R. Shreiber, "Results of an Experiment to Measure the Velocity of Sound in Foam," *Sov. Phys. Acoust.* **38**, 1–4 (1992).
- Verbist, G., D. Weaire and A. M. Kraynik, "The Foam Drainage Equation," *J. Phys.: Condens. Matter* **8**, 3715–3731 (1996).
- Weaire, D., S. Findlay and G. Verbist, "Measurement of Foam Drainage using AC Conductivity," *J. Phys.: Condens. Matter* **7**, L217–L222 (1995).
- Wenzel, H. G., R. J. Brungraber, and T. E. Stelson, "The Viscosity of High Expansion Foam," *J. Mater.* **5**, 396–412 (1970).
- Wood, A. B., *A Textbook of Sound* (Bell, London, 1941).
- Yoshimura, A. S., R. K. Prud'homme, H. M. Princen and A. D. Kiss, "A Comparison of Techniques for Measuring Yield Stresses," *J. Rheol.* **31**, 699–710 (1987).